

## Research Results

# Compact Dual Band Bandpass Microstrip Filter with Open End Line Resonators for WiMAX and WLAN Applications

Satyendra Kumar<sup>1</sup>, Dr. Ratnesh Kumar Jain<sup>2</sup>

<sup>1</sup>M.Tech. Research Scholar, Department of Electronics & Communication, RKDF University, Bhopal (M.P)

<sup>2</sup>Research Guide, Department of Electronics & Communication, RKDF University, Bhopal (M.P)

### ABSTRACT

In recent decades, the rapid expansion of wireless and mobile communication has evolved in a progressively cluttered electromagnetic spectrum as a result of fast rise of these technologies. In the communications industry, compact passband filters with great performance are in high demand due to their small size. There is currently a lot of research and development going on to find new ways to make microstrip filters that are smaller and more efficient.

This work proposed a compact bandpass filter with two open end line resonators for WLAN and WiMAX applications. The physical size of the filter is 25×16 mm<sup>2</sup>. The filter has full ground structure and substrate is made of FR4 material having 4.3 dielectric constant and 1.6 mm thickness. The filter is made of two open end line resonators and two open end line stubs. Resonators and Stubs are arranged in symmetrical manner to the filter geometry around y-axis. Proposed dual band bandpass filter is having negative group delay which increases the use of filter in potential and practical applications of microwave systems. The filter has passband characteristics on 5.02, and 9.87GHz with the insertion loss of 0.83dB, and 1.48dB having return loss of 41.8dB, 30.3dB, 20.45dB, and 18.35dB. Filter exhibits good fractional bandwidth of 34.78%, 17.12%, 8.55%, 6.2%, and 3.83% respectively. Proposed filter has 2 transmission zeros. The tested and simulated results of  $|S_{11}|$  and  $|S_{21}|$  parameters are near similar which shows the good agreement of design parameters.

### KEYWORDS

Dual-band, Bandpass filter, microstrip filter, NGD, open end line resonators, line stub, WLAN, WiMAX.

## 1. INTRODUCTION

When IEEE 802.11b/g (GSM), 802.11a (WLAN), GPS, RFID, 3G/ 4G/ Bluetooth and vehicle radar systems are integrated, the requirement for a small wireless transceiver for commercial goods is even greater [1]. These wireless technologies, as described in [2,] need high data rates and a considerable amount of radio frequency spectrum capacity.

In addition to mobile phones, radio frequency systems are required for scientific instruments, navigation, and even medicinal applications. To avoid interfering with other radio frequency bands, efforts are being made to design a small, low-power component for wireless standards. Compact, high-selectivity bandpass filters are an essential part of this system since their performance affects the overall performance of the microwave communication system. Circuit designers have a significant difficulty in designing multiband BPFs with small footprints and minimal insertion loss in order to accomplish this goal. To improve upper stopband performance and provide an outstanding pass band feature in the UWB region, microstrip lines may exhibit notch bands [4]. A resonator is often used in filter designs in order to get the desired working band, which allows the filter to be smaller [5]. A

faulty ground structure like that described in [6] may be a better option for increasing the sharpness of the scattering characteristics. Metamaterial significantly reduces the filter's physical profile, as shown by [7]. Because of their size and great loss properties, hybrid forms like circular rings and rectangular stubs are an ideal choice.

The FCC-recommended frequency range in [1] while rejecting unwanted signals outside of the provided range, and to design and build a BPF with an appropriate fundamental topology to achieve this goal. GSM 1900, WLAN, WiMAX C-band and X-band BPFs are constructed using thick rectangular stubs [8-10], which increase the passband's edge steepness and overall performance while reducing its size. [8-10] When used in WiMAX and WLAN, C-band and X-band satellite applications [11-15], it is connected to thin I-shaped rectangular stubs with centrally loaded twin small inverted-Y stubs to provide quad band responses at 1.918 MHz and 2.411 MHz and 4.06 GHz [11-15]. The design idea is evaluated on a FR4 substrate material to ensure that the suggested samples are viable. Relative permittivity is 4.3, and the filter substrate has a dissipation factor of 0.002. It is possible to open and short-circuit the different shaped stubs on the filters in order to modify their configuration and centre frequency [17]. In

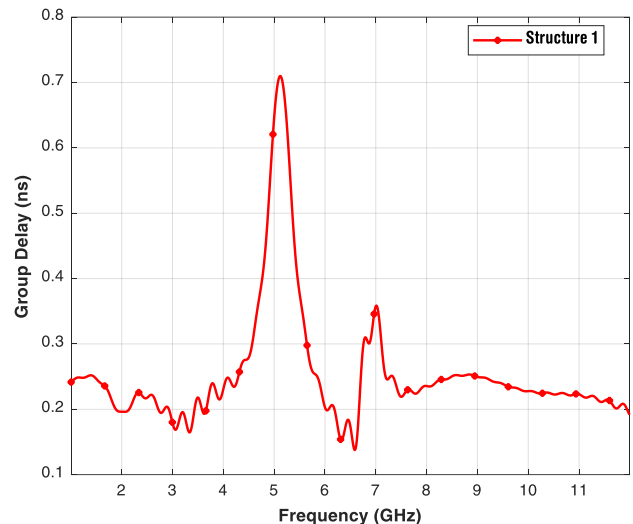
terms of microwave applications, a filter with a negative group delay is very versatile and widely used [18]. Compared to single band or dual band filters, multiband band pass filters provide a variety of benefits [19-21]. Open end line resonators with a symmetrical arrangement are used in the suggested filter design to provide dual-band band-pass operation.

## 2. PROPOSED DUAL BAND FILTER DESIGN AND RESONATOR ANALYSIS

The fundamental dual-band filter configuration with line stubs with its corresponding S-parameter frequency plot is depicted in Figure 1(a). The scattering parameters of first stage design has been discussed in this section. The overall volume of the proposed filter is  $25 \times 16 \times 1.6 \text{ mm}^3$  where left edge of the filter has port  $P_1$  (input) and right edge has port  $P_2$  (output).

### 2.1 Analysis of Structure1

In the first design structure the filter has rectangular feedline along with thin line stub placed in parallel with the symmetrical feedline of opposite port refer to Figure 1(a). The port is kept little bit larger height than feed line symmetrical to x-axis. The return loss and insertion loss characteristics of the filter are shown in Figure 1(b) after the excitation. There are two stop bands exhibited by this given structure and it resonates on passband frequencies of 3.387GHz and 6.852GHz. This design has only two Transmission Zeros (TZs). The group delay of Structure1 is shown in Figure 1(c) and has positive delay throughout the simulated range from 1-12GHz.

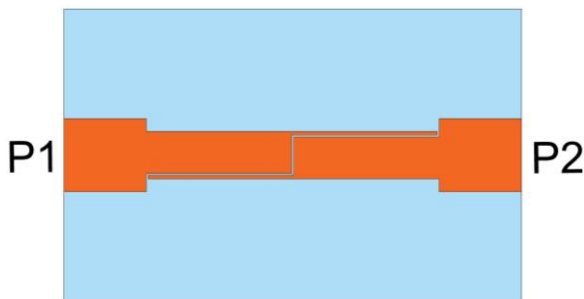


(c)

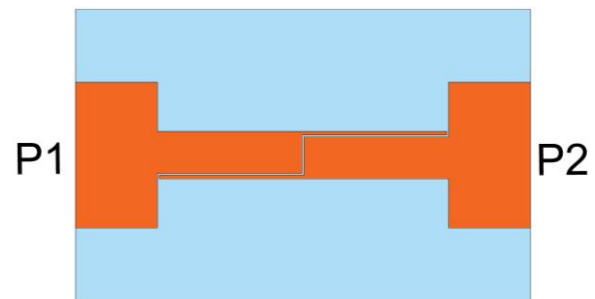
Figure 1. (a) Layout of the Filter Structure 1, (b) S-parameter curves of Structure 1 and (c) Group Delay of Structure 1

### 2.2 Analysis of Structure2

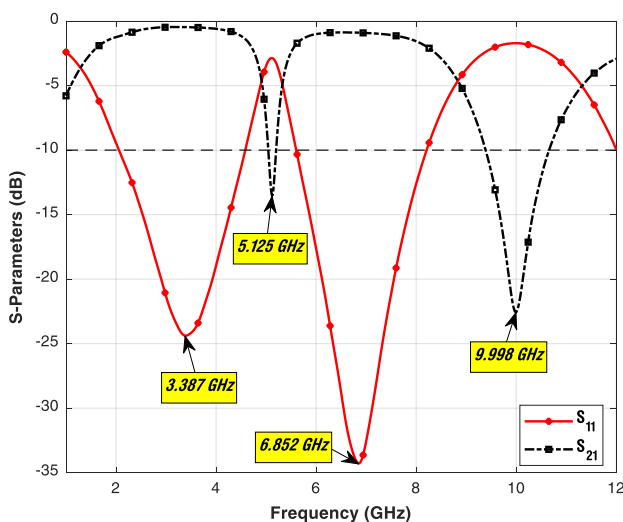
First structure needs some optimization to get near our goal for wireless applications. So, some changes in the design have been incorporated to found Structure2 of the filter. In this design height of the ports 1 and 2 of the filter is increased rest of the elements like feedline and thin line stubs are kept same. The geometry has been depicted in Figure 2(a). The return loss and insertion loss characteristics of the filter are shown in Figure 2(b) after the excitation.



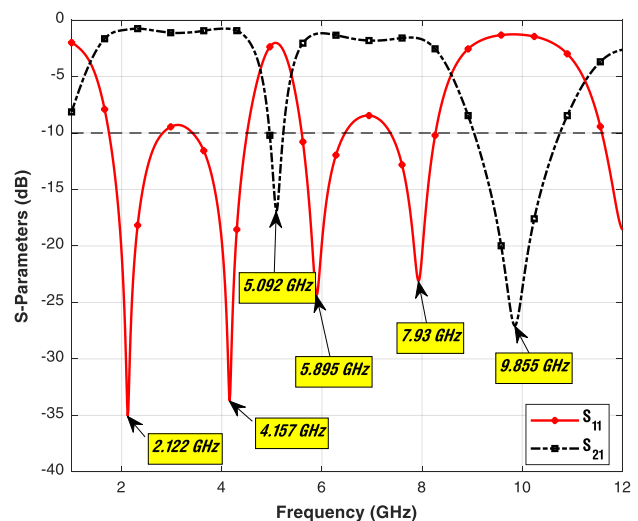
(a)



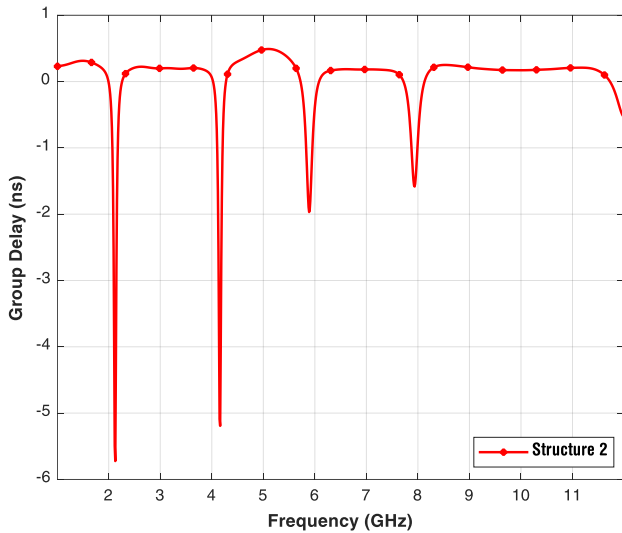
(a)



(b)



(b)



(c)

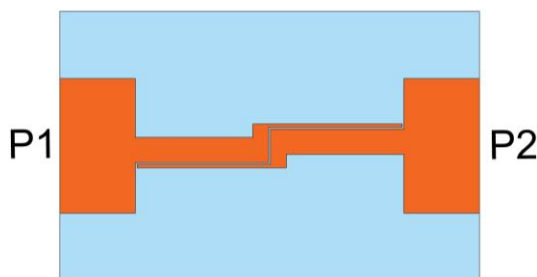
Figure 2. (a) Layout of the Filter Structure2, (b) S-parameter curves of Structure2 and (c) Group Delay of Structure2

There are two stop bands exhibited by this Structure2 between 1 to 11GHz and it resonates on 5.092GHz, and 9.855GHz. After modification in the port's height symmetrically along y axis, filter starts resonating on four frequencies 2.122GHz, 4.157GHz in passband 1, 5.895GHz, 7.93GHz in passband 2. In comparison with previous structure the passband  $S_{11}$  characteristics divided into two bands in passband. This structure also has two TZs. The group delay of Structure2 is shown in Figure 2(c) and has negative delay throughout the simulated range from 1-12GHz.

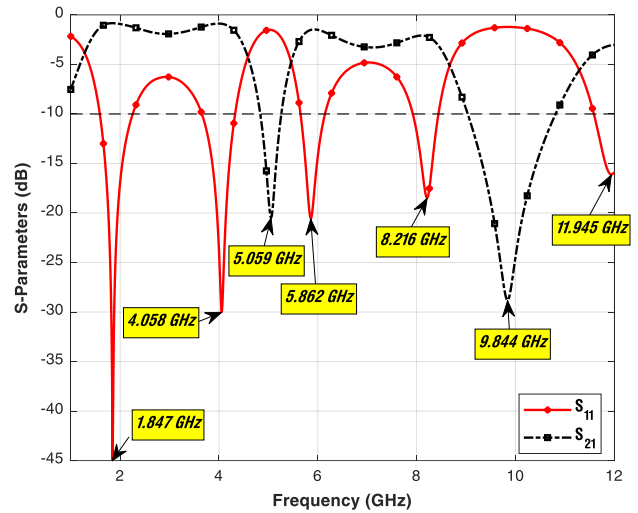
### 2.3 Analysis of Structure3

For the sake of more precise results second structure needs have performed some optimizations. These changes have been incorporated to find Structure3 of the filter. In this design height of the ports 1 and 2 of the filter is kept as Structure2 and the feedline has been introduced with the incorporation of rectangular slot in the feedline of width  $W_F$  and height  $L_F$ . The geometry has been depicted in Figure 3(a). The return loss and insertion loss characteristics of the filter are shown in Figure 3(b) after the excitation.

There are two stop bands exhibited by this Structure3 between 1 to 11GHz and it resonates on 5.059GHz, and 9.844GHz. By making slots the pass band frequencies of  $S_{11}$  parameter are 1.847GHz, 4.058GHz, 5.862GHz and 8.216GHz. Number of TZs are two in this structure. The group delay of Structure3 is shown in Figure 3(c) and has negative delay on passband resonating frequencies in the simulated range from 1-12GHz.

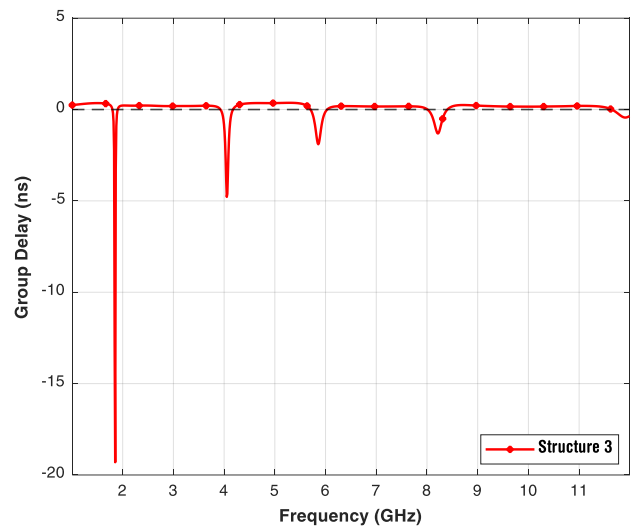


(a)



Resonance Frequency fr1 = 1.847 GHz  
Resonance Frequency fr2 = 4.058 GHz  
Resonance Frequency fr3 = 5.862 GHz  
Resonance Frequency fr4 = 8.216 GHz  
Resonance Frequency fr5 = 11.945 GHz  
Resonance Frequency fr1 = 5.059 GHz  
Resonance Frequency fr2 = 9.844 GHz

(b)



(c)

Figure 3. (a) Layout of the Filter Structure3, (b) S-parameter curves of Structure2 and (c) Group Delay of Structure2

### 2.4 Analysis of Structure4 (Final Filter Geometry)

The final geometry of the filter is achieved as Structure4 after tuning the passband resonance frequencies for consumer wireless application like WiMAX and WLAN. The tuning in the Structure3 has been done by adding two symmetrical line resonators placed in parallel to the open-end line stubs. The dimensions of the resonators are of  $W_R$  width and  $L_R$  height. The geometry of the final filter design is shown in Figure 4(a) and the geometry with detailed dimension is shown in Figure 6(a). The return loss and insertion loss characteristics of the Structure4 are shown in Figure 4(b) after the excitation.

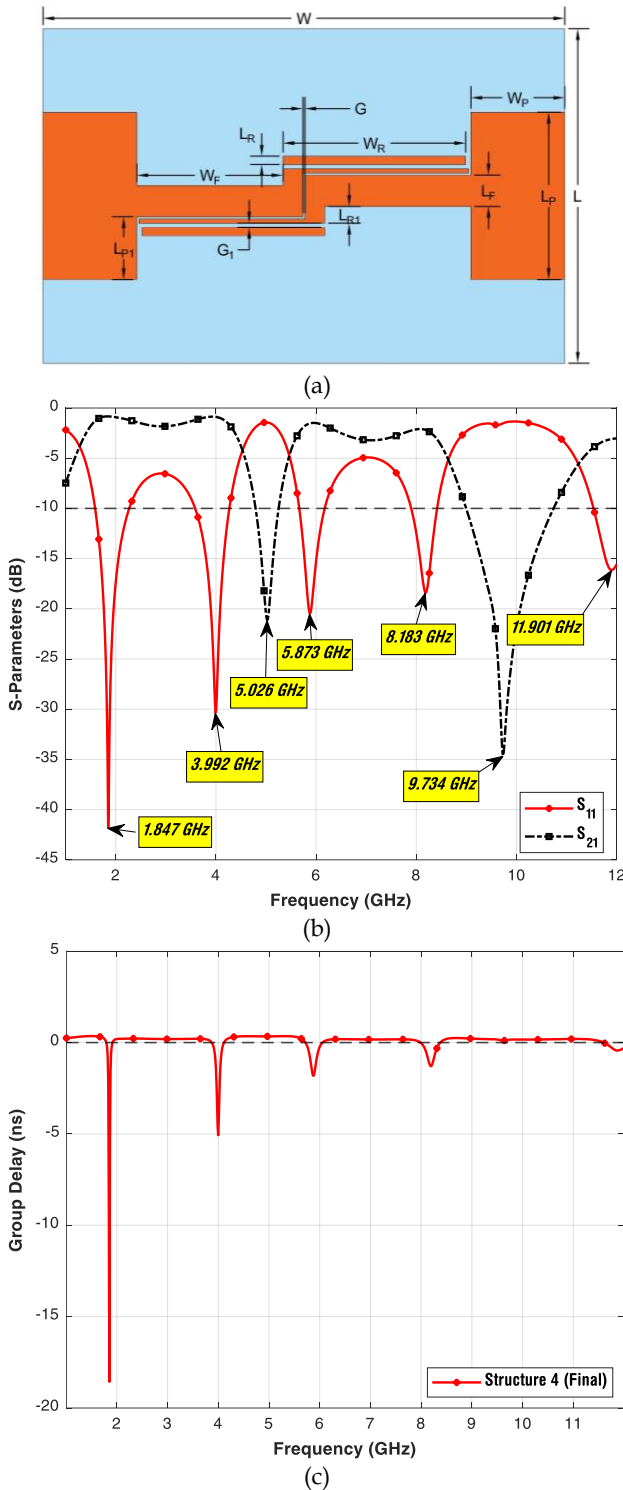


Figure 4. (a) Optimized Geometry of the Presented Filter Structure 4, (b) S-parameter curves of Structure 4 and (c) Group Delay of Structure 4

The final pass bands have been seen by this Structure 4 between 1 to 11GHz and it resonates on 5.026GHz, and 9.734GHz. By adding line resonators, the pass band frequencies of  $S_{11}$  parameter are shifted to 1.847GHz, 3.992GHz, 5.873GHz and 8.183GHz. Number of TZs are two in this structure. The group delay of Structure 4 is shown in Figure 4(c) and has negative delay on passband resonating frequencies in the simulated range from 1-12GHz.

The comparison of the return loss and insertion loss characteristics of the filter structure evolution has been compared and shown in Figure 5.

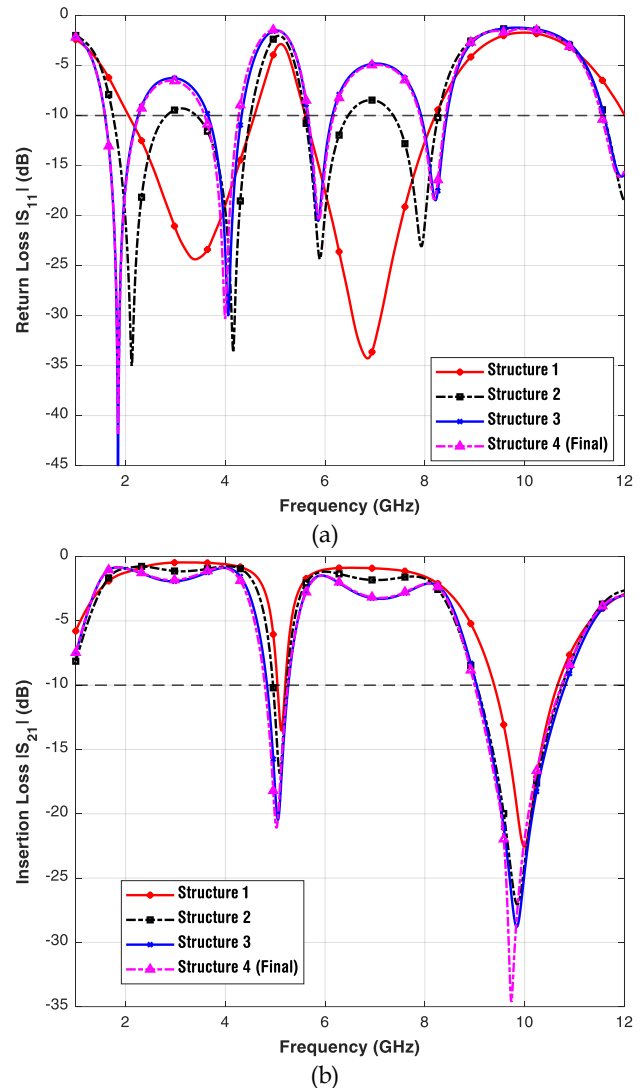


Figure 5. S-Parameter comparison of Structure 1 to 4 (a) Return Loss (b) Insertion Loss

Finally, the overall structure of proposed filter along with all stubs and resonators are shown in Figure 6(a). The detailed designed

Table 1. Dimension of Filter

Dimension	Value (mm)	Dimension	Value (mm)
$W$	25	$L$	16
$W_P$	4.5	$L_P$	8
$W_R$	8.75	$L_{P1}$	3
$W_F$	7	$L_F$	1.5
$G$	0.1	$L_R$	0.4
$G_1$	0.2	$L_{R1}$	0.8

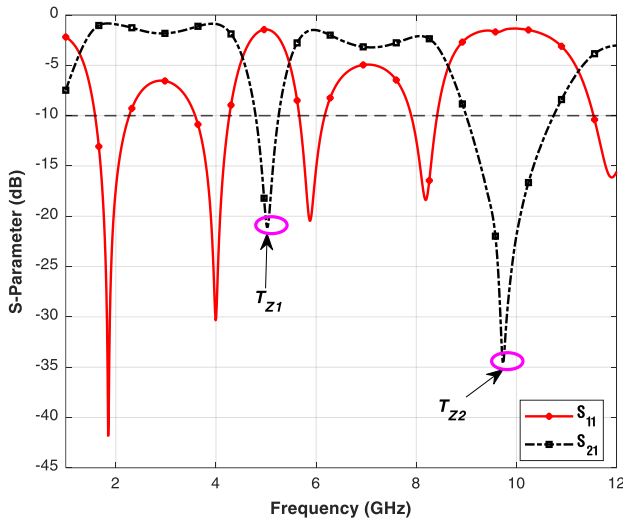


Figure6. All TZs of the proposed filter

### 3. EXPERIMENTAL RESULT ANALYSIS

Figure 7 depicts the picture of realized dual band filter prototype based on line stubs and open-end line resonators placed symmetrically. Physical size of this bandpass filter is just (25×16) mm<sup>2</sup>, making it compact than prior designs [15-16],[18],[20] and [23-24].

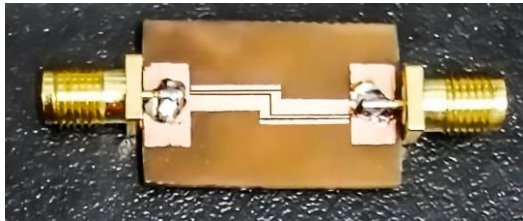


Figure 7. Picture of Realized Fabricated Filter

Table 2. Characteristics comparison of simulation vs measured outcomes of dual band filter

	Passband (GHz)	Insertion Loss (dB)	Return Loss (dB)	FBW (%)	TZ
Simulation	1.93/3.92/5.92/8.16	0.8/1.48	47/31/21/17	34.78/17.12/8.55/6.2	2
Measured	1.85/3.9/6.03/8.06	1.2/0.6	29/18/19/16	43.3/16.9/8.5/6.02	2

Table 3. Performance comparison of filter with previous works

Ref.	Passband (GHz)	Insertion Loss (dB)	Return Loss (dB)	FBW (%)	Size (mm <sup>2</sup> )/( $\lambda_g \times \lambda_g$ )
[6]	7.5	1.2	12	100	26mm×20mm
[8]	7.8	0.4/0.8	19/15	116	34mm × 12mm 0.06×0.02
[9]	1.3/2.06	0.55/0.66	26/23	6/3	24mm ×24mm
[15]	2.5/3.4/4.12-5.32	0.37/0.09/0.05	11/19/23	12/21/25	40mm×30.44mm
[18]	1.995	7.5	> 20	-	60mm × 36mm 0.58×0.35
[20]	1.575/2.4/3.45	0.7/1.14/0.3	18/22.3/17	15.8/7.5/5.6	38mm×31mm
[22]	2.5/3.8	½	23/25	8/5.2	20mm ×30mm
[23]	1.51/2.13/2.8	0.74/1.29/1.41	50/25/27	12/7.3/7	108mm × 65mm
Proposed	1.85/3.9/6.03/8.06	1.2/0.6	29/18/19/16	43.3/16.9/8.5/6.02	25mm ×16mm

The suggested filter's reflection coefficient ( $|S_{11}|$ ) and insertion loss ( $|S_{21}|$ ) were tested using an Anritsu vector network analyser.

Figure 8 shows a comparison of the proposed filter's measured and simulated return loss characteristics. It is a graph that compares the experimented and simulated return loss scattering parameters for proposed dual band filter with two symmetrical identical line stubs and line resonators. As shown in Figure 8, the experimental performance has a maximum return loss of -29dB in the pass-band and the simulated response has reflection coefficient of -41.8dB in the pass-band. For the target frequency band, both simulated and measured results are in good agreement.

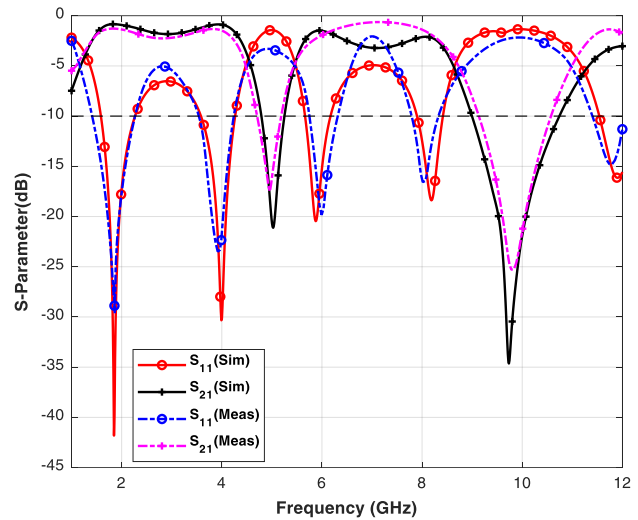


Figure 8. Scattering parameter of the quad band filter simulation and measured



Figure 8 also shows a comparison between measured and simulated  $|S_{21}|$  characteristics. It is a graph comparing the observed and calculated insertion loss for proposed quadband filter with line stubs and resonators. The calculated performance corresponds to a maximum attenuation of -34.5dB in the stop-band, while the measured response corresponds to an enhanced maximum attenuation of -25.5dB in the stop-band. Figure 6 shows the group delay of the proposed filter, which is in negative. Due to NGD the proposed bandpass filter can be implemented in the feed-forward amplifier circuits and feedback amplifiers which enhances the performance [18] and reduce the physical profile of the circuit.

Table 2 gives the detailed findings of scattering parameters ( $|S_{11}|$ ;  $|S_{21}|$ ) among simulated and measured outcomes e.g., passband, insertion loss, return loss, fractional bandwidth and transmission zeros of the proposed dual band filter using two identical line resonators and open-end line stubs.

The proposed dual band filter has comparison of performance metrics with previous filter realizations given in Table 3. Proposed filter design has dual bands of operation while maintaining lower physical profile of 25×16 mm<sup>2</sup>. The fractional bandwidth is better than [9], [15],[20] and [22].

#### 4. CONCLUSION AND FUTURE SCOPE

Great-performance passband filters are in high demand in communications because they are small and work well. Researchers are looking at new ways to construct compact microstrip filters in order to boost their performance and shrink their overall filter size. We were able to create and test a small filter design in this piece of work. It may be inferred that the suggested filter design can function for four bands based on the results of the experiment. According to Table 3, it is also smaller than its rivals in terms of physical dimensions. This work provided a two open end line stub and two line resonators dual band bandpass filter for WLAN and WiMAX applications. The filter's dimensions are 25 mm × 16 mm. The substrate is made of FR4 and has a dielectric constant of 4.3 and a thickness of 1.6 millimeters. Asymmetry is avoided by aligning the resonators and stubs in the same direction. The negative group delay of the dual band bandpass filter under consideration makes it more suitable for use in microwave systems. On 1.85GHz, 3.9GHz, 6.03GHz, and 8.06GHz, insertion loss is 1.2dB and 0.6dB, while return loss is 29, 18, 19, 16dB. Fractional bandwidths of 43.3%, 16.9%, 8.5%, and 6.02 percent are all good for the filter. Two TZs are suggested for use in the filter. An excellent agreement in the design parameters may be shown by comparing the measured and predicted return and insertion loss values. The DGS technique may be used to further improve this design by adjusting the frequency of desired processes. Pass and stop bands may be added by integrating resonators. Furthermore, the device's size may be further reduced by the use of a different substrate material. It is possible to use the suggested bandpass filter in the feed-forward amplifier and feedback amplifier circuits, which improves performance and reduces the circuit's physical profile.

#### REFERENCES

- [1] FCC, 'Revision of part 15 of the commission's rules regarding ultra-wideband transmission systems'. Tech. Rep. ETDocket 98-153, FCC02-48, Federal Communications Commission, 2002.
- [2] T. George and B. Lethakumary, 'High frequency rejection using L shaped defected microstrip structure in ultra wideband bandpass filter', *Materials Today: Proceedings*, vol. 25, pp. 265-268, 2020, doi: [10.1016/j.matpr.2020.01.363](https://doi.org/10.1016/j.matpr.2020.01.363).
- [3] C.-Y. Hung, M.-H. Weng, Y.-K. Su, R.-Y. Yang, and H.-W. Wu, 'Design of Compact and Sharp-Rejection Ultra Wideband Bandpass Filters Using Interdigital Stepped-Impedance Resonators', *IEICE Transactions on Electronics*, vol. E90-C, no. 8, pp. 1652-1654, Aug. 2007, doi: [10.1093/ietele/e90-c-8.1652](https://doi.org/10.1093/ietele/e90-c-8.1652).
- [4] S. W. Wong and L. Zhu, 'Implementation of Compact UWB Bandpass Filter With a Notch-Band', *IEEE Microw. Wireless Compon. Lett.*, vol. 18, no. 1, pp. 10-12, Jan. 2008, doi: [10.1109/LMWC.2007.911972](https://doi.org/10.1109/LMWC.2007.911972).
- [5] A. Belmajdoub, A. E. Alami, S. Das, B. T. P. Madhav, S. D. Bennani, and M. Jorio, 'Design, optimization and realization of compact bandpass filter using two identical square open-loop resonators for wireless communications systems', *J. Inst.*, vol. 14, no. 09, pp. P09012-P09012, Sep. 2019, doi: [10.1088/1748-0221/14/09/P09012](https://doi.org/10.1088/1748-0221/14/09/P09012).
- [6] J. Liu, W. Ding, J. Chen, and A. Zhang, 'New Ultra-Wideband Filter with Sharp Notched Band Using Defected Ground Structure', *PIER Letters*, vol. 83, pp. 99-105, 2019, doi: [10.2528/PIERL18111302](https://doi.org/10.2528/PIERL18111302).
- [7] D. K. Choudhary and R. K. Chaudhary, 'A Compact via-Less Metamaterial Wideband Bandpass Filter Using Split Circular Rings and Rectangular Stub', *PIER Letters*, vol. 72, pp. 99-106, 2018, doi: [10.2528/PIERL17092503](https://doi.org/10.2528/PIERL17092503).
- [8] A. Basit, M. I. Khattak, and M. Alhassan, 'Design and Analysis of a Microstrip Planar UWB Bandpass Filter with Triple Notch Bands for WiMAX, WLAN, and X-Band Satellite Communication Systems', *PIER M*, vol. 93, pp. 155-164, 2020, doi: [10.2528/PIERM20042602](https://doi.org/10.2528/PIERM20042602).
- [9] C. Karpuz, A. K. Gorur, and E. Sahin, 'Dual-mode dual-band microstrip bandpass filter with controllable center frequency', *Microw. Opt. Technol. Lett.*, vol. 57, no. 3, pp. 639-642, Mar. 2015, doi: [10.1002/mop.28914](https://doi.org/10.1002/mop.28914).
- [10] R. Gomez-Garcia, J.-M. Munoz-Ferreras, W. Feng, and D. Psychogiou, 'Balanced Symmetrical Quasi-Reflectionless Single-and Dual-Band Bandpass Planar Filters', *IEEE Microw. Wireless Compon. Lett.*, vol. 28, no. 9, pp. 798-800, Sep. 2018, doi: [10.1109/LMWC.2018.2856400](https://doi.org/10.1109/LMWC.2018.2856400).
- [11] L.-T. Wang, Y. Xiong, L. Gong, M. Zhang, H. Li, and X.-J. Zhao, 'Design of Dual-Band Bandpass Filter With Multiple Transmission Zeros Using Transversal Signal Interaction Concepts', *IEEE Microw. Wireless Compon. Lett.*, vol. 29, no. 1, pp. 32-34, Jan. 2019, doi: [10.1109/LMWC.2018.2884147](https://doi.org/10.1109/LMWC.2018.2884147).
- [12] R. Gomez-Garcia, L. Yang, J.-M. Munoz-Ferreras, and D. Psychogiou, 'Selectivity-Enhancement Technique for Stepped-Impedance-Resonator Dual-Passband Filters', *IEEE Microw. Wireless Compon. Lett.*, vol. 29, no. 7, pp. 453-455, Jul. 2019, doi: [10.1109/LMWC.2019.2916458](https://doi.org/10.1109/LMWC.2019.2916458).
- [13] B. Ren et al., 'Compact Dual-Band Differential Bandpass Filter Using Quadruple-Mode Stepped-Impedance Square Ring Loaded Resonators', *IEEE Access*, vol. 6, pp. 21850-21858, 2018, doi: [10.1109/ACCESS.2018.2829025](https://doi.org/10.1109/ACCESS.2018.2829025).
- [14] M.-H. Weng, S.-W. Lan, S.-J. Chang, and R.-Y. Yang, 'Design of Dual-Band Bandpass Filter With Simultaneous Narrow- and Wide-Bandwidth and a Wide Stopband', *IEEE Access*, vol.

- 7, pp. 147694-147703, 2019, doi: [10.1109/ACCESS.2019.2946302](https://doi.org/10.1109/ACCESS.2019.2946302).
- [15] T. A. Sheikh, J. Borah, and S. Roy, 'Design of compact bandpass filter for WiMAX and UWB application using asymmetric SIRS and DGS', *Radioelectron.Commun.Syst.*, vol. 59, no. 6, pp. 269-273, Jun. 2016, doi: [10.3103/S0735272716060066](https://doi.org/10.3103/S0735272716060066).
- [16] M. Mabrok, Z. Zakaria, Y. E. Masrukin, T. Sutikno, and H. Alsariera, 'Effect of the defected microstrip structure shapes on the performance of dual-band bandpass filter for wireless communications', *Bulletin EEI*, vol. 10, no. 1, pp. 232-240, Feb. 2021, doi: [10.11591/eei.v10i1.2662](https://doi.org/10.11591/eei.v10i1.2662).
- [17] G.-Z. Liang and F.-C. Chen, 'A Compact Dual-Wideband Bandpass Filter Based on Open-/Short-Circuited Stubs', *IEEE Access*, vol. 8, pp. 20488-20492, 2020, doi: [10.1109/ACCESS.2020.2968518](https://doi.org/10.1109/ACCESS.2020.2968518).
- [18] Z. Wang, Z. Fu, C. Li, S.-J. Fang, and H. Liu, 'A Compact Negative-Group-Delay Microstrip Bandpass Filter', *PIER Letters*, vol. 90, pp. 45-51, 2020, doi: [10.2528/PIERL19122701](https://doi.org/10.2528/PIERL19122701).
- [19] Z. Gao, P. Wu, and Y. Zhang, 'A New Compact Microstrip Ultra-Wideband (UWB) Bandstop Filter with Good Performance', *PIER Letters*, vol. 93, pp. 9-12, 2020, doi: [10.2528/PIERL20052304](https://doi.org/10.2528/PIERL20052304).
- [20] M. Rahman and J.-D. Park, 'A Compact Tri-Band Bandpass Filter Using Two Stub-Loaded Dual Mode Resonators', *PIER M*, vol. 64, pp. 201-209, 2018, doi: [10.2528/PIERM17120404](https://doi.org/10.2528/PIERM17120404).
- [21] K. G. Avinash and I. Srinivasa Rao, 'Compact dual-band bandpass filter based on dual-mode modified star shaped resonator', *Microw. Opt. Technol. Lett.*, vol. 59, no. 3, pp. 505-511, Mar. 2017, doi: [10.1002/mop.30333](https://doi.org/10.1002/mop.30333).
- [22] C. Kim, T. Hyeon Lee, B. Shrestha, and K. Chul Son, 'Miniaturized dual-band bandpass filter based on stepped impedance resonators', *Microw. Opt. Technol. Lett.*, vol. 59, no. 5, pp. 1116-1119, May 2017, doi: [10.1002/mop.30481](https://doi.org/10.1002/mop.30481).
- [23] R. Gomez-Garcia, R. Loeches-Sanchez, D. Psychogiou, and D. Peroulis, 'Multi-Stub-Loaded Differential-Mode Planar Multiband Bandpass Filters', *IEEE Trans. Circuits Syst. II*, vol. 65, no. 3, pp. 271-275, Mar. 2018, doi: [10.1109/TCSII.2017.2688336](https://doi.org/10.1109/TCSII.2017.2688336).
- [24] Z. Yang, B. You, and G. Luo, 'Dual-/tri-band bandpass filter using multimode rectangular SIW cavity', *MicrowOpt Technol Lett*, vol. 62, no. 3, pp. 1098-1102, Mar. 2020, doi: [10.1002/mop.32145](https://doi.org/10.1002/mop.32145).
- [25] F. Zhao, M. Weng, C. Tsai, R. Yang, H. Lai, and S. Liu, 'A miniaturized high selectivity band-pass filter using a dual-mode patch resonator with two pairs of slots', *MicrowOpt Technol Lett*, vol. 62, no. 3, pp. 1145-1151, Mar. 2020, doi: [10.1002/mop.32165](https://doi.org/10.1002/mop.32165).